

1 **Assessing Climate Change Impacts on Live Fuel Moisture and Wildfire Risk**
2 **Using a Hydrodynamic Vegetation Model**

3 Wu Ma¹, Lu Zhai², Alexandria Pivovarov³, Jacquelyn Shuman⁴, Polly Buotte⁵, Junyan Ding⁶, Bradley
4 Christoffersen⁷, Ryan Knox⁶, Max Moritz⁸, Rosie A. Fisher⁹, Charles D. Koven⁶, Lara Kueppers¹⁰,
5 Chonggang Xu^{1,*}

6 ¹*Earth and Environmental Sciences Division, Los Alamos National Laboratory, Los Alamos,*
7 *NM, United States*

8 ²*Department of Natural Resource Ecology and Management, Oklahoma State University,*
9 *Stillwater, OK, United States*

10 ³*Atmospheric Science and Global Change Division, Pacific Northwest National Laboratory,*
11 *Richland, WA, United States*

12 ⁴*National Center for Atmospheric Research, Climate and Global Dynamics, Terrestrial Sciences*
13 *Section, Boulder, CO, United States*

14 ⁵*Energy and Resources Group, University of California, Berkeley, CA, United States*

15 ⁶*Climate and Ecosystem Sciences Division, Lawrence Berkeley National Laboratory, CA, United*
16 *States*

17 ⁷*Department of Biology, University of Texas Rio Grande Valley, Edinburg, TX, United States*

18 ⁸*UC ANR Cooperative Extension, Bren School of Environmental Science & Management,*
19 *University of California, Santa Barbara, CA, United States*

20 ⁹*Centre Européen de Recherche et de Formation Avancée en Calcul Scientifique, Toulouse,*
21 *France*

22 ¹⁰*Energy and Resources Group, University of California, Berkeley, and Lawrence Berkeley*
23 *National Laboratory, Berkeley, CA, United States*

24

25 * *Corresponding author (Chonggang Xu, cxu@lanl.gov)*

26 **Abstract:** Live fuel moisture content (LFMC) plays a critical role in wildfire dynamics, but little
27 is known about responses of LFMC to multivariate climate change, e.g., warming temperature,
28 CO₂ fertilization and altered precipitation patterns, leading to a limited prediction ability of
29 future wildfire risks. Here, we use a hydrodynamic demographic vegetation model to estimate
30 LFMC dynamics of chaparral shrubs, a dominant vegetation type in fire-prone southern
31 California. We parameterize the model based on observed shrub allometry and hydraulic traits,
32 and evaluate the model's accuracy through comparisons between observed and simulated LFMC
33 of three plant functional types (PFTs) under current climate conditions. Moreover, we estimate
34 the number of days per year of LFMC below 79% (which is a critical threshold for wildfire
35 danger rating of southern California chaparral shrubs) from 1960 to 2099 for each PFT, and
36 compare the number of days below the threshold for medium and high greenhouse gas emission
37 scenarios (RCP4.5 and 8.5). We find that climate change could lead to more days per year (5.2-
38 14.8% increase) with LFMC below 79% between the historical (1960-1999) and future (2080-
39 2099) periods, implying an increase in wildfire danger for chaparral shrubs in southern
40 California. Under the high greenhouse gas emission scenario during the dry season, we find that
41 the future LFMC reductions mainly result from a warming temperature, which leads to 9.1-
42 18.6% reduction in LFMC. Lower precipitation in the spring leads to a 6.3-8.1% reduction in
43 LFMC. The combined impacts of warming and precipitation change on fire season length are
44 equal to the additive impacts of warming and precipitation change individually. Our results show
45 that the CO₂ fertilization will mitigate fire risk by causing a 3.5-4.8% increase in LFMC. Our
46 results suggest that multivariate climate change could cause a significant net reduction in LFMC
47 and thus exacerbate future wildfire danger in chaparral shrub systems.

48 **Keywords:** FATES-HYDRO, chaparral shrubs, plant functional types, southern California, CO₂
49 enrichment, climate change

50 **1. Introduction**

51 Historical warming and changes in precipitation have already impacted wildfire at a
52 global scale (e.g. Stocks et al. 1998; Gillett et al. 2004; Westerling et al. 2003, 2006) and it is
53 expected that accelerating future warming will continue to significantly influence global wildfire
54 regimes (e.g. Flannigan et al. 2009; Liu et al. 2010; Moritz et al. 2012). So far, prior studies have
55 mainly focused on impacts of dead fuel moisture, fuel loads, and weather conditions on wildfire.
56 Limited studies have applied proxies of live fuel moisture in global-fire models. For example,
57 dead fuel moisture is found to be related to fire ignition and fire spread potential (or potential
58 area burnt) (Aguado et al. 2007), specific weather conditions such as increased vapor pressure
59 deficit (Williams et al. 2019) can lead to a vast increase in fire activity (Goss et al. 2020), and
60 wildfire fuel loads are projected to increase under climate change (Matthews et al. 2012; Clarke
61 et al. 2016). In global-fire models, studies have used proxies of live fuel moisture (Bistinas et al.
62 2014; Kelley et al. 2019) as well as explicit representation of live fuels (Hantson et al. 2016;
63 Rabin et al. 2017). While previous studies provide great insights into fire risks with changes in
64 climate, dead fuel moisture, fuel loads, and representation of live fuel moisture, there is still
65 limited understanding of how climate change influences live fuel moisture content (LFMC) and
66 the consequent wildfire risks. This is particularly true for the combined impacts of warming
67 temperature, altered precipitation, and increasing CO₂ fertilization (Chuvieco et al. 2004;
68 Pellizzaro 2007; Caccamo et al. 2012a, b; Williams et al. 2019; Goss et al. 2020).

69 A measure of water content within living plant tissue in relation to their dry weight,
70 LFMC has been found to be one of the most critical factors influencing combustion, fire spread,

71 and fire consumption (e.g. Agee et al. 2002; Zarco-Tejada et al. 2003; Bilgili & Saglam 2003;
72 Yebra et al. 2008; Dennison et al. 2008; Anderson & Anderson 2010; Keeley et al. 2011). This is
73 because a low LFMC leads to increased flammability and a higher likelihood of ignition
74 (Dimitrakopoulos & Papaioannou 2001). For instance, LFMC was found to be a significant
75 factor contributing to the occurrence of wildfires in Australia (Plucinski 2003; Nolan et al. 2016;
76 Yebra et al. 2018; Rossa & Fernandes 2018; Pimont et al. 2019), Spain (Chuvieco et al. 2009)
77 and California (Santa Monica Mountains; Dennison et al. 2008; Dennison & Moritz 2009;
78 Pivovarovff et al. 2019). Dennison & Moritz (2009) found strong evidence of a LFMC threshold
79 (79%) for southern California chaparral shrubs, which may determine when large fires can occur
80 in this region.

81 Vegetation moisture content is dependent on both ecophysiological characteristics of the
82 species and environmental conditions, including both climatic variables and soil water
83 availability (Rothermel 1972; Castro et al. 2003; Castro et al. 2003; Pellizzaro 2007; Pivovarovff
84 et al. 2019; Nolan et al. 2020). So far, little is known about the relative importance of different
85 climate variables to future LFMC dynamics. On the one hand, warming could contribute to a
86 higher atmospheric demand and higher evapotranspiration (Rind et al. 1990) and thus lead to a
87 lower LFMC. On the other hand, higher CO₂ concentration will decrease stomatal conductance
88 (Wullschleger et al. 2002) and plant water loss, and thus lead to a higher LFMC. The impacts of
89 CO₂ and warming could be complicated by local changes in precipitation patterns and humidity
90 (Mikkelsen et al. 2008).

91 The sensitivity of LFMC to climate change is likely to be affected by plant hydraulic
92 traits (the plant properties that regulate water transport and storage within plant tissues), which
93 affect plant water regulation (Wu et al. 2020). Variations in hydraulic traits reflect contrasting

94 plant drought adaptation strategies when responding to dry conditions. Two contrasting overall
95 strategies are: 1) water stress avoiders and 2) water stress tolerators (Tobin et al. 1999; Wei et al.
96 2019). The “avoiders” are generally characterized by a more conservative hydraulic strategy
97 under water stress by either closing stomata early, dropping leaves or accessing deep water to
98 avoid more negative water potentials and therefore xylem cavitation. Meanwhile, the “tolerators”
99 typically build xylem and leaves that are more resistant to cavitation so that they can tolerate
100 more negative water potential and continue to conduct photosynthesis under water stress.
101 Therefore, compared with the tolerators, the avoiders normally have a lower sapwood density
102 and higher plant water storage capacity in their tissues to avoid cavitation (Meinzer et al. 2003,
103 2009; Pineda-Garcia et al. 2013). Because the avoiders rely on water storage capacity as one way
104 to avoid cavitation thereby maintaining a relatively high LFMC, and water loss from storage
105 should increase with warming, LFMC could be more sensitive to climate change in avoiders
106 relative to tolerators.

107 While over half of terrestrial landscapes on Earth are considered fire-prone (Krawchuk et
108 al. 2009), Mediterranean-type climate regions are routinely impacted by fire, often on an annual
109 basis. This is partly because Mediterranean climate regions are characterized by winter rains
110 followed by annual dry season, when little to no rainfall occurs for several months. Multiday
111 periods of extreme high temperatures, as well as katabatic hot, dry, and intense winds, often
112 punctuate the annual drought, leading to some of the worst fire weather in the world (Schroeder
113 et al. 1964). This can result in wildfires that are large, high-intensity, and stand-replacing
114 (Keeley 1995; Keeley & Zedler 2009; Balch et al. 2017). Globally, Mediterranean climate
115 regions are characterized by evergreen sclerophyllous-leaved shrublands. The Mediterranean
116 climate region in California is dominated by chaparral, which is adapted to the periodic fire

117 regime in California (Venturas et al. 2016). Previous studies have proposed a variety of
118 relationships between chaparral LFMC and fire danger in southern California (Dennison et al.
119 2008; Dennison & Moritz 2009), but less is known about how climate changes could alter LFMC
120 and fire danger. In chaparral, LFMC is usually high during the winter and spring (wet season)
121 and then gradually declines during the dry season (summer and fall), which leads to a typical fire
122 season approximately six months long in southern California (Pivovaroff et al. 2019). One key
123 risk is that severe drought conditions are becoming exacerbated under climate change, which
124 might lead to the occurrence of larger and higher-intensity fires in chaparral (Dennison et al.
125 2008; Dennison & Moritz 2009).

126 There has been a long history of wildfire modeling, with three types of models: 1) fine-
127 scale fire behavior models (e.g. FIRETEC by Linn et al. 2002); 2) landscape-scale fire
128 disturbance models (e.g. LANDIS-II by Sturtevant et al. 2009); and 3) global-scale fire dynamics
129 models (e.g. Hantson et al. 2016; Rabin et al. 2017; SPITFIRE by Thonicke et al. 2010). While
130 these models focus on simulation at different scales, fire measures of the simulation are mainly
131 calculated from climate and dead fuel moisture and currently lack prediction of LFMC dynamics.
132 One key limitation is that most previous models have not yet considered plant hydrodynamics
133 (Holm et al. 2012; Xu et al. 2013; Seiler et al. 2014), which is integral to LFMC prediction.
134 Recently, there have been important improvements to global dynamic and demographic
135 vegetation models by incorporating plant hydrodynamics (McDowell et al. 2013; Xu et al. 2016;
136 Fisher et al. 2018; Mencuccini et al. 2019). These models have been used to study the interaction
137 between elevated CO₂ and drought (Duursma & Medlyn, 2012), the impact of hydraulic traits on
138 plant drought response (Christofferson et al. 2016), the role of hydraulic diversity in vegetation
139 response to drought (Xu et al. 2016) and hydroclimate change (Powell et al. 2018), and

140 vegetation water stress and root water uptake (Kennedy et al. 2019). While the main purpose of
141 the new hydraulic components is to improve the vegetation response to drought, the fact that
142 hydrodynamic models consider tissue water content as a prognostic variable provides an
143 opportunity to assess the climate impacts on LFMC.

144 The objective of this study is to quantify LFMC dynamics and associated changes in fire
145 season duration for a chaparral ecosystem in southern California under climate change using a
146 vegetation demographic model (that resolves the size and age-since-disturbance structure of
147 plant populations) (Xu et al. 2016; Fisher et al. 2018) that incorporates plant hydraulics. We test
148 one overarching hypothesis: future climate change will decrease LFMC and consequently result
149 in a longer fire season as determined by a critical threshold of LFMC (H_0). Specifically, we test
150 the following four sub-hypotheses: 1) warming has a stronger impact on LFMC than CO_2
151 fertilization (H_1); 2) the reductions in spring and autumn precipitation lead to a longer fire season
152 as determined by LFMC (H_2); 3) the combined impacts of warming and precipitation on fire
153 season length are equal to the additive impacts of warming and precipitation change individually
154 (H_3); and 4) LFMC for plants with more conservative hydraulic strategies (“avoiders”) will be
155 more vulnerable to warming (H_4).

156 **2. Materials and Methods**

157 To understand climate change impacts on LFMC for the chaparral ecosystem, we applied
158 the Functionally Assembled Terrestrial Simulator (FATES; Fisher et al. 2015; Massoud et al.
159 2019; Koven et al. 2020) coupled with a hydrodynamic vegetation module (FATES-HYDRO;
160 Christoffersen et al. 2016) in the Santa Monica Mountains in California. We validated the model
161 using the observed LFMC for three chaparral shrub plant functional types (PFTs). Then, we
162 applied FATES-HYDRO to estimate long-term dynamics of leaf water content (LWC) during

163 1960-2099 for each PFT using downscaled Earth System Model (ESM) climate scenarios. We
164 converted simulated leaf water content (LWC) to LFMC within leaves and shoots. Based on the
165 simulated LFMC, we evaluated wildfire danger based on the number of days per year of LFMC
166 below the critical value of 79% from 1960 to 2099 for each PFT under RCP 4.5 and 8.5. Finally,
167 we assessed the relative importance of changes in individual and combined climate variables
168 including CO₂, temperature, precipitation, and tested the corresponding hypotheses.

169 **2.1 Study site**

170 The study site is located at the Stunt Ranch Santa Monica Mountains Reserve, in the
171 Santa Monica Mountains in California, USA (N 34° 05', W 118° 39'). Stunt Ranch is dominated
172 by chaparral vegetation, with an elevation of approximately 350 m, a west-facing slope, and a
173 Mediterranean-type climate. The study site harbors an abundance of fauna, particularly birds and
174 reptiles. The mean annual temperature is 18.1°C. The mean annual precipitation is 478 mm,
175 occurring mostly during the wet season (i.e. November-March) with almost no rainfall during the
176 dry season (i.e. April-October). Stunt Ranch last burned in year 1993. We focused on PFTs
177 representing 11 study species (Fig. 1), including chamise (*Adenostoma fasciculatum* - Af), red
178 shank (*Adenostoma sparsifolium* - As), big berry manzanita (*Arctostaphylos glauca* - Ag), buck
179 brush (*Ceanothus cuneatus* - Cc), greenbark ceanothus (*Ceanothus spinosus* - Cs), mountain
180 mahogany (*Cercocarpus betuloides* - Cb), toyon (*Heteromeles arbutifolia* - Ha), laurel sumac
181 (*Malosma laurina* - Ml), scrub oak (*Quercus berberidifolia* - Qb), hollyleaf redberry (*Rhamnus*
182 *ilicifolia* - Ri), and sugar bush (*Rhus ovata* - Ro). Detailed information about the study site and
183 species characterizations found at Stunt Ranch can be found in Venturas et al. (2016) and
184 Pivovaroff et al. (2019).

185 **2.2 FATES-HYDRO model**

186 FATES is a vegetation demographic model (Fisher et al. 2015), which uses a size-
187 structured group of plants (cohorts) and successional trajectory-based patches based on the
188 ecosystem demography approach (Moorcroft et al. 2001). FATES simulates the demographic
189 process including seed production, seed emergence, growth and mortality (Koven et al. 2020).
190 Because the main purpose is to assess LFMC, we controlled for variation in plant size structure
191 that could arise from plant traits or climate differences between model runs by using a reduced-
192 complexity configuration of the model where growth and mortality are turned off and ecosystem
193 structure is held constant. FATES has to be hosted by a land surface model to simulate the soil
194 hydrology, canopy temperature and transpiration. These host land models include the Exascale
195 Energy Earth System Model (E3SM, Caldwell et al., 2019) land model (ELM) as well as the
196 Community Earth System Model (Fisher et al 2015) and the Norwegian Earth system model
197 (NorESM, Tjiputra et al 2013). In this study, we used the DOE-sponsored ELM as our host land
198 model. The time step of FATES to calculate carbon and water fluxes is 30 minutes and it can
199 downscale the data from 6-hourly climate drivers.

200 A key component of FATES, the plant hydrodynamic model (HYDRO, based on
201 Christoffersen et al. 2016), simulates the water flow from soil through root, stem and leaf to the
202 atmosphere. In this model, water flow is calculated based on water pressure gradients across
203 different plant compartments (leaf, stem, transporting roots, absorbing roots and rhizosphere).
204 Specifically, flow between compartment i and $i + 1$ (Q_i) is given by

$$Q_i = -K_i \Delta h_i, \quad (1)$$

205 where K_i is the total conductance ($\text{kg MPa}^{-1} \text{s}^{-1}$) at the boundary of compartments i and $i + 1$ and
206 Δh_i is the total water potential difference between the compartments:

$$\Delta h_i = \rho_w g (z_i - z_{i+1}) + (\psi_i - \psi_{i+1}), \quad (2)$$

207 where z_i is compartment distance above (+) or below (-) the soil surface (m), ρ_w is the density of
 208 water (10^3 kg m^{-3}), g is acceleration due to gravity (9.8 m s^{-2}), and ψ_i is tissue or soil matric
 209 water potential (MPa). K_i is treated here as the product of a maximum boundary conductance
 210 between compartments i and $i + 1$ ($K_{max,i}$), and the fractional maximum hydraulic conductance
 211 of the adjacent compartments (FMC_i or FMC_{i+1}), which is a function of the tissue water content.
 212 A key parameter that controls FMC is the critical water potential (P_{50}) that leads to 50% loss of
 213 hydraulic conductivity. The tissue water potential is calculated based on pressure-volume (PV)
 214 theory (Tyree & Hammel, 1972; Tyree & Yang, 1990; Bartlett et al., 2012). For leaves, it is
 215 described by three phases: 1) capillary water phase with full turgor, 2) elastic drainage phase
 216 before reaching turgor loss point; and 3) post-turgor loss phase. For other tissues, it only has
 217 phases 2 and 3. Compared to a non-hydrodynamic model, this formulation allows the simulation
 218 of plant water transport limitation on transpiration. For the non-hydrodynamic version of
 219 FATES, the water limitation factor for transpiration (B_{tran}) is calculated based on the soil
 220 moisture potential (Fisher et al. 2015). For the hydrodynamic version, B_{tran} is calculated based on
 221 the leaf water potential (ψ_l) (Christoffersen et al. 2016) as follows,

$$B_{tran} = [1 + (\frac{\psi_l}{P_{50_gs}})^{a_l}]^{-1} \quad (3)$$

223 where P_{50_gs} is the leaf water potential that leads to 50% loss of stomatal conductance and a_l is
 224 the shape parameter. Please refer to Christoffersen, et al. 2016 for details of formulations of
 225 FMC for different plant tissues.

226 **2.3 Allometry and trait data for model parameterization**

227 FATES-HYDRO has a large number of parameters (>80; see Massoud et al. 2019 for a
228 complete list except for hydraulic parameters). Based on a previous sensitivity analysis study
229 (Massoud et al. 2019), we focused our parameter estimation efforts on the most influential
230 parameters for allometry, leaf and wood traits, and hydraulic traits from observations of 11
231 chaparral shrub species (see Supplementary, Table S2), collected from Jacobsen et al. (2008) and
232 Venturas et al. (2016). For this study, we assumed that the allometry of a shrub is analogous to
233 that of a small tree. However, we did make several important modifications to accommodate the
234 allometry of shrub as their height and crown area relationships to diameter could be different
235 from trees. First, instead of using the diameter at breast height as the basis for allometry to
236 calculate the height, crown area and leaf biomass, we used the basal diameter as the basis for
237 shrubs. Second, in the allometry of trees, the diameter for maximum height (d_1 :
238 `Fates_allom_dbh_maxheight`, Table S1) is the same as the diameter for maximum crown area (d_2 :
239 `Fates_allom_d2ca_max`, Table S1). As our data showed that d_1 and d_2 are different for shrubs,
240 we have modified the codes so that the d_1 and d_2 can be set for different values. It is possible that
241 different branching and path length patterns for stems of chaparral species could impact the
242 hydraulics compared to trees; however, FATES-HYDRO treats all the aboveground xylem as a
243 single pool and thus it should not affect our model simulation results.

244 Based on a hierarchical cluster analysis (Bridges 1966) of allometry and trait data, there
245 are a clear separation among the shrub species. First, the dendrogram is built and every data
246 point finally merges into a single cluster with the height shown on the y-axis. Then we cut the
247 dendrogram in order to create the desired number of clusters determined by a pragmatic choice
248 based on hydraulic traits of eleven chaparral shrub species (Fig. 1). R's `rect.hclust` function
249 (<https://www.rdocumentation.org/packages/stats/versions/3.6.2/topics/rect.hclust>) was used to

250 see the clusters on the dendrogram. All parameters of allometry, leaf and wood traits, and
251 hydraulic traits were collected from observations shown in the Table S2 and S3 of the
252 supplementary. According to the principle of model parsimony, we do not want to classify the
253 species into more than 3 PFTs. Meanwhile, we also want to differentiate the fundamental plant
254 growth and water use strategies that will determine plant transpiration rate and the corresponding
255 LFMC. If we choose to classify the species into two PFTs (based on the solid horizontal line in
256 Fig. 1), then we will not be able to differentiate species with aggressive and conservative
257 hydraulic strategies in the second group and not be able to test H4. Therefore, the chaparral shrub
258 species were classified into three PFTs (based on the dotted horizontal line in Fig. 1 and Table
259 S3), that are able to differentiate plant growth and hydraulic strategy. The three PFTs include a
260 low productivity, aggressive drought tolerance hydraulic strategy PFT (PFT-LA) with a relative
261 low $V_{c,max25}$ (the maximum carboxylation rate at 25 °C) and a very negative P_{50} (the leaf water
262 potential leading to 50% loss of hydraulic conductivity); a medium productivity, conservative
263 drought tolerance hydraulic strategy PFT (PFT-MC) represented by a medium $V_{c,max25}$ and a less
264 negative P_{50} , turgor loss point and water potential at full turgor; and a high productivity,
265 aggressive drought tolerance hydraulic strategy PFT (PFT-HA) with a relatively high $V_{c,max25}$
266 and a very negative P_{50} . The mean of species-level trait data weighted by species abundance at
267 the site were used to parameterize FATES-HYDRO.

268 **2.4 Model initialization**

269 Our model simulation is transient in terms of soil water content, leaf water content,
270 carbon and water fluxes. The forest structure (plant sizes and number density) is fixed and is
271 parameterized based on a vegetation inventory from Venturas et al. (2016). The soil texture and
272 depth information are parameterization based on a national soil survey database

273 (<https://websoilsurvey.sc.egov.usda.gov/App/WebSoilSurvey.aspx>; Table S1). The soil moisture
274 is initialized with 50% of the saturation and the tissue plant water content is initialized so that it
275 is in equilibrium with the soil water potential. We run the model for 10 years based on 1950-
276 1960 climate so that the simulated soil moisture, leaf water content, carbon and water fluxes are
277 not depending on their initial conditions.

278 **2.5 Live Fuel Moisture Content for model validation**

279 In this study, we used measured LFMC to validate simulated LFMC. FATES-HYDRO
280 does not directly simulate the LFMC. Thus, we estimated the LFMC based on simulated LWC.
281 The LWC in the model is calculated as follows,

$$282 \quad \text{LWC} = \frac{fw-dw}{dw} * 100, \quad (4)$$

283 where, fw is the fresh weight and dw is the dry weight, which are simulated within FATES-
284 HYDRO. Then, we estimated the LFMC within leaves and shoots (< 6 mm diameter) using the
285 empirical equation derived from shrub LFMC and LWC data including the three regenerative
286 strategies [seeder (S), resprouter (R) and seeder–resprouter (SR)], in summer, autumn and winter
287 from Fig. 4 and 5 in Saura-Mas and Lloret’s study (2007) as follows (Fig. S4),

$$288 \quad \text{LFMC} = 31.091 + 0.491\text{LWC}, \quad (5)$$

289 The climate in Saura-Mas and Lloret’s study is Mediterranean (north-east Iberian Peninsula),
290 which is consistent with the climate of our study area. LFMC was measured on our site
291 approximately every three weeks, concurrently with plant water potentials in 2015 and 2016.
292 LFMC measurement details can be found in Pivovarov et al. (2019). For comparison with our
293 model outputs, we calculated the mean LFMC within leaves and shoots for each PFT weighted

294 by the species abundance (Venturas et al. 2016). Species abundance was calculated by dividing
295 mean density of a specific species by the mean density of all species.

296 **2.6 Climate drivers**

297 We forced the FATES-HYDRO model with 6-hourly temperature, precipitation,
298 downward solar radiation, and wind components. Historical climate data during 2012-2019,
299 which were used for FATES-HYDRO calibration, were extracted from a local weather station
300 (<https://stuntranch.ucnrs.org/weather-date/>). Historical and future climate data during 1950-2099,
301 which were used for simulations of LFMC by FATES-HYDRO model, were downloaded from
302 the Multivariate Adaptive Constructed Analogs (MACA) datasets (Abatzoglou & Brown 2012;
303 <http://maca.northwestknowledge.net>). The MACA datasets (1/24-degree or approximately 4-km;
304 Abatzoglou & Brown 2012) include 20 ESMs with historical forcings during 1950-2005 and
305 future Representative Concentration Pathways (RCPs) RCP 4.5 and RCP8.5 scenarios during
306 2006-2099 from the native resolution of the ESMs. The gridded surface meteorological dataset
307 METDATA (Abatzoglou, 2013) were used with high spatial resolution (1/24-degree) and daily
308 timescales for near-surface minimum/maximum temperature, precipitation, downward solar
309 radiation, and wind components. Then we downscaled the MACA daily data to 6-hourly based
310 on the temporal anomaly of the observed mean daily data to the hourly data for each day during
311 2012-2019. The model is driven by yearly CO₂ data obtained from Meinshausen et al (2011).

312 **2.7 Hypothesis testing**

313 To test H₀ (future climate change will decrease LFMC and consequently result in a longer
314 fire season as determined by a critical threshold of LFMC), we compared the simulated mean
315 LFMC, derived from modeled leaf water content, under the climate projections from 20 ESMs

316 under RCP 4.5 and 8.5. We then tested if the LFMC during the April-October dry season in the
317 historic period of 1960-1999 is significantly higher than that in the future period of 2080-2099.
318 For the fire season duration, we estimated the number of days per year below a critical threshold
319 of LFMC (79%). Similarly, we tested if the number of days per year below the critical threshold
320 of LFMC during the historical period are significantly different from that during the future
321 period. We used a bootstrapped approach (Jackson 1993) to test if the mean of LFMC or fire
322 season duration are significantly different between these two periods. Specifically, we randomly
323 draw 10000 samples from the simulated residuals of LFMCS or fire season durations estimated
324 by 20 ESMs for these two periods under the null hypothesis that there is no difference in the
325 mean. We then calculated p-values by comparing the simulated mean difference to the empirical
326 distribution of difference estimated from these 10000 samples. See Supplementary section 5.2
327 within Xu et al. (2019) for the details.

328 To test H_1 (warming has a stronger impact on LFMC than CO_2 fertilization), we
329 compared mean simulated LFMC and fire season length for three PFTs with/without CO_2
330 changes (fixed CO_2 at 367 ppm vs dynamic CO_2 concentrations from RCP 4.5 or RCP 8.5) and
331 warming. To remove the future warming trend, future temperature was replaced with historical
332 (1986-2005) temperature data for every 20 year period. Similarly, to test H_2 (the reductions in
333 spring and autumn precipitation lead to a longer fire season as determined by LFMC), we
334 compared the model outputs of LFMC and fire season length for three PFTs with/without
335 precipitation changes. To test H_3 (the combined impacts of warming and precipitation on fire
336 season length are equal to the additive impacts of warming and precipitation change
337 individually), we compared model outputs of LFMC and fire season length for three PFTs under
338 three scenarios: 1) without warming; 2) without precipitation changes; and 3) without warming

339 and precipitation changes. Finally, to test H₄ (LFMC for plants with more conservative hydraulic
340 strategies will be more vulnerable to warming), we compared model outputs of LFMC and fire
341 season length across the three different PFTs with different hydraulic strategies.

342 **3. Results**

343 **3.1 Comparison between simulated and measured LFMC**

344 Our results showed that FATES-HYDRO was able to capture variation in the LFMC for
345 different PFTs and soil water content in 5-cm depth (Fig. 2 and S3), also for Chamise in 2018
346 (Fig. S5) although we had limited observed LFMC data. Specifically, the model was able to
347 capture 96%, 86%, and 80% of the variance in observed LFMC for the period of 2015-2016 for
348 three PFTs, respectively (Fig. 2 b, d, f). The model was also able to capture the seasonal
349 dynamics of soil water content, LFMC, and LFMC below the threshold 79% in comparison to
350 observed data (Fig. 2 a, c, e and S3). To validate that FATES-HYDRO is able to capture the
351 interannual variability of LFMC, we compared the simulated LFMC for PFT-LA with the long-
352 term observations of LFMC for the chamise species (*Adenostoma fasciculatum*; Fig. S5). Our
353 results showed that the model is able to reasonably capture the seasonal and interannual
354 variability for the period of 2006-2019 ($R^2=0.7$), although it underestimates peaks in LFMC in 4
355 of 14 years.

356 **3.2 Changes in the LFMC and fire season length from historical to future periods**

357 Using the validated model driven by climate projections from 20 ESMs under greenhouse
358 gas emission scenarios RCP4.5 and RCP 8.5, we found that the daily mean LFMC during the
359 future period of 2080-2099 was projected to become significantly lower than that during the
360 historical period of 1960-1999 for all three PFTs (Fig 3, $P<0.000001$). Our results also showed

361 that the spread among models increase with time, suggesting a larger uncertainty in the
362 projection into the future. Specifically, the histogram of daily mean LFMC during the April-
363 October dry season showed that there was a higher probability of low LFMC under future
364 climate conditions (Fig. S1). The daily mean LFMC decreased from 84.7%, 101.3%, and 78.4%
365 during the historical period of 1960-1999 to 81.0-82.8%, 96.3-98.8%, and 74.8-76.6% during the
366 future period of 2080-2099 under both climate scenarios for PFT-LA, PFT-MC, PFT-HA,
367 respectively (Fig 3).

368 Based on the projected LFMC, there was a significant increase in the fire season length
369 with the critical threshold of LFMC from the historical period of 1960-1999 to the future period
370 of 2080-2099 for three PFTs. With the critical threshold of 79% LFMC, the fire season length
371 was projected to increase by 20, 22, 19 days under RCP 8.5 (Fig. 4 and Table S4), and to
372 increase by 9, 11, 8 days under RCP 4.5 (Fig. 4 and Table S4). Our results also showed that the
373 spread among models increase with time, suggesting a larger uncertainty in the projection into
374 the future. The above results for mean LFMC and fire season length support hypothesis H₀ that
375 future climate change will decrease LFMC and consequently result in a longer fire season, as
376 determined by critical thresholds for LFMC, for all three PFTs.

377 **3.3 Relative effects of individual climate changes on the length of the fire season**

378 In order to better understand the relative contribution to fire season length of different
379 climate variables, we ran FATES-HYDRO for three PFTs using meteorological forcings that
380 isolated and removed changes in individual specific variables. Our results showed that the
381 increase in fire season length mainly resulted from warming, which led to 16-23 days (9.1-
382 18.6%) per year increase in fire season length for the critical threshold of 79% LFMC under RCP
383 8.5 (Fig. 5). This is because warming is pushing Vapor Pressure Deficit (VPD) higher, resulting

384 in increased fire season length. For RCP 4.5, the warming contributed to 5-6 days (3.8-4.3%) per
385 year increase in fire season length (Fig. 5). We also found that elevated CO₂ concentrations
386 decreased fire season length with 6-7 days (3.5-4.8%) per year decrease in fire season length
387 under RCP 8.5 (Fig. 5). Under RCP 4.5, CO₂ increases led to 2-3 days (1.5-2.2%) per year
388 decrease in fire season length (Fig. 5). Because the impact of warming on fire season length was
389 stronger than the mitigation from CO₂ enrichment, our results support hypothesis H₁ (warming
390 has a stronger impact on LFMC than CO₂ fertilization).

391 Even though total precipitation was projected to increase in the future, lower precipitation
392 in the spring and autumn (Fig. S2 a, b) led to 8-10 days (6.3-8.1%) per year increase in fire
393 season length with the critical threshold of 79% LFMC under RCP 8.5 (Fig. 5). Under RCP 4.5,
394 the precipitation changes contributed to 1-3 days (0.8-1.6%) increase in fire season length (Fig.
395 5). This result supported hypothesis H₂ that the reductions in spring and autumn precipitation
396 lead to a longer fire season as determined by LFMC.

397 Our results showed that the combined impacts of warming and precipitation on fire
398 season length were equal to the additive impacts of warming and precipitation change
399 individually. This supported hypothesis H₃. Specifically, the combined changes in temperature
400 and precipitation caused 24-33 days per year (15.6-26.8%) increase in fire season length with the
401 critical threshold of 79% LFMC under RCP 8.5 (Fig. 5). Under RCP 4.5, the combined changes
402 in temperature and precipitation caused a 6-9 days per year (4.8-6.1%) change in fire season
403 length.

404 **3.4 Comparison of changes in fire season length among three PFTs under climate change**

405 Regarding three PFTs under both climate scenarios, fire season length of PFT-HA was
406 the longest (167-176 days per year), while fire season length of PFT-MC was the shortest (114-
407 124 per year) during 2080-2099 (Fig. 4). However, the response of fire season length to warming
408 was strongest for PFT-MC. Specifically, for PFT-MC, warming under RCP 8.5 led to an increase
409 of 21.6% (22 days) in fire season length (Fig. 5 b) and warming under RCP 4.5 led to an increase
410 of 10.8% (11 days) in fire season length. For PFT-LA, warming under RCP 8.5 led to an increase
411 of 14.7% (19 days) in fire season length (Fig. 5 a) while warming under RCP 4.5 led to an
412 increase of 7.4% (9 days) in fire season length. Finally, for PFT-HA, warming under RCP 8.5 led
413 to an increase of 10.2% (18 days) in fire season length (Fig. 5 c) and 5.3% (8 days) in fire season
414 length with under RCP 4.5. Because PFT-MC has a more conservative hydraulic strategy with
415 less negative P_{50} , turgor loss point and water potential at full turgor, this result supported
416 hypothesis H₄ that the LFMC for plants with more conservative hydraulic strategy will be more
417 vulnerable to warming.

418 To validate our classification scheme, we compared these PFT-level results to those
419 obtained with single-PFT and 2-PFT simulations finding that using the three PFTs defined by our
420 cluster analysis gives a qualitatively different view of LFMC change than a single- or 2-PFT
421 simulation. We found **significant differences in the percentage changes of LFMC and fire season**
422 **length between future period (2080-2099) and historical period (1960-1999) using three distinct**
423 **PFTs, but no significant differences between PFTs in 2-PFT simulations under the different**
424 **climate scenarios (Fig. S6).**

425 **4. Discussion**

426 Low LFMC within shrub leaves and shoots increases the flammability and likelihood of
427 combustion, making it vitally important to monitor temporal variations in LFMC, especially

428 during the dry season (Dennison et al, 2008). The strong relationships between observed and
429 simulated LFMC of all PFTs (Fig. 2) suggested that the plant hydrodynamic model, FATES-
430 HYDRO, could accurately estimate LFMC seasonal dynamics as a function of modeled leaf
431 water content, and consequently be useful to predict fire risks in Mediterranean-type climate
432 regions, although only small amount of validation data were used and the underlying assumption
433 that a shrub was analogous to a small tree. Based on the simulated monthly mean LFMC during
434 2006-2019 for PFT-LA, which includes the chamise species, we found that our model can
435 capture the seasonal variation and interannual variability, but underestimates the highest wet
436 season peaks in LFMC in 4 of 14 years (Fig. S5). This may cause biases for future projections
437 while it would not highly affect the long-term trend of LFMC and fire season length. During the
438 future period (2080-2099) and the historical period (1960-1999), both periods displayed lower
439 values in the dry season (April - October), which is consistent with lower LFMC during the
440 summer-fall dry season, rather than the winter-spring wet season (Chuvieco et al, 2004;
441 Pellizzaro et al, 2007; Pivovarovoff et al. 2019). Extremely low daily LFMC was more likely to
442 occur during the future period, which had higher temperature than the historical period. From the
443 historical to the future period, fire season length could increase by 5.2-14.8% under climate
444 change for chaparral shrub ecosystems (H₀). The fire season length was not validated, rather it
445 was defined as number of days with LFMC below 79%.

446 Quantifying influences of climatic variables on LFMC is crucial to predicting future fire
447 risks (Dennison & Moritz, 2009). Our results showed that future warming was the most
448 important driver of LFMC. This finding suggested that warming would substantially push Vapor
449 Pressure Deficit (VPD) higher and decrease LFMC and strongly increase the fire season length,
450 which may greatly increase fire risks in the future (e.g. Dennison et al, 2008; Chuvieco et al,

451 2009; Pimont et al, 2019). CO₂ fertilization is expected to reduce stomatal conductance (Pataki et
452 al. 2000; Tognetti et al. 2000) and thus could mitigate the impacts of warming on LFMC. Our
453 results illustrated that, even though the CO₂ impact did cause a 3.5-4.8% reduction in fire season
454 length, the impact of warming on fire season length is about 5.6-13.8% larger than the CO₂ effect
455 (H₁, warming has a stronger impact on LFMC than CO₂ fertilization). This result suggests that
456 CO₂ fertilization cannot offset the LFMC impacts from warming. The FATES-HYDRO model
457 assumes a consistent stomatal sensitivity to CO₂ concentration across Mediterranean shrub
458 species. While Mediterranean shrub functional types in arid and semi-arid systems would vary in
459 their stomatal response in the real world (Pataki et al. 2000). Therefore, our model may
460 overestimate/underestimate the CO₂ effect on stomatal conductance and its mitigating influence
461 might be smaller in reality for some species.

462 Previous studies implied that the timing of precipitation may have a strong impact on
463 subsequent LFMC (e.g. Veblen et al. 2000; Westerling et al. 2006; Dennison & Moritz 2009). In
464 this study, precipitation was also a key driver of LFMC under future climate conditions. Our
465 results showed that, even though total precipitation was projected to increase, the reduction in
466 spring and autumn precipitation (Fig. S2) was projected to cause a longer fire season length (H₂,
467 the reductions in spring and autumn precipitation lead to a longer fire season as determined by
468 LFMC; Fig. 5). This result was in agreement with a prior study indicating that spring
469 precipitation, particularly in the month of March, was found to be the primary driver of timing of
470 LFMC changes (Dennison & Moritz 2009). We also found that the combined impacts of
471 warming and precipitation on fire season length were equal to the linearly additive impacts of
472 warming and precipitation change individually (H₃). Our results suggested that, when evaluating

473 future fire risks, it is critical that we considered the seasonal changes in precipitation and its
474 interaction with the warming impact.

475 Modeled vegetation responses to environmental changes is a function of variation in plant
476 functional traits (Koven et al, 2020). The three PFTs represented in this study have similar
477 patterns in LFMC in response to climate change during 1960-2099, but we did see some critical
478 differences. Specifically, the plant functional type PFT-MC with more conservative hydraulic
479 strategy had the strongest responses to climate change (Fig. 5). This could be related to the fact
480 that the PFT-MC is a more conservative drought tolerant PFT in terms of hydraulic strategy with
481 less negative P_{50} , turgor loss point, and water potential at full turgor. The PFT-MC plants had a
482 relatively high saturated water content based on observed data (Fig 2) and the water within plant
483 tissues thus changes more quickly in response to the environmental condition changes (H4,
484 LFMC for plants with more conservative hydraulic strategies will be more vulnerable to
485 warming). However, the three different PFTs were coexisting at the same location in model
486 simulations, coexistence and heterogeneity in LFMC might impact fire behavior and fire season
487 length.

488 Because the moisture content of live fuels (~50–200%) are much higher than that of dead
489 fuels (~7–30%), leaf senescence induced by drought stress and subsequent mortality are
490 potentially vital factors to cause large wildfires (Nolan et al. 2016, 2020). Thus drought-induced
491 canopy die-back and mortality could largely increase surface fine fuel loads and vegetation
492 flammability, which can increase the probability of wildfire (Ruthrof et al. 2016). Since growth
493 and mortality are turned off in model runs by using a reduced-complexity configuration, it is
494 possible that vegetation density might decrease and LFMC could be conserved under future
495 scenarios. In addition, potential vegetation transitions (e.g., shrubs to grassland and species

496 composition changes) might substantially affect flammability and thus fire intensity and
497 frequency. In this study, we used the static mode of FATES-HYDRO to simulate LWC dynamics
498 under climate change. If we need to assess how the leaf senescence and vegetation dynamics will
499 impact the fire behavior, we can use the same model with dynamic mode to assess their impacts
500 on fire behaviors under future drought and warming conditions.

501 Application of a hydrodynamic vegetation model to estimate LFMC dynamics could
502 potentially benefit wildfire modeling at the fine-scale, landscape-scale, and global-scale. This is
503 because LFMC is one of the most critical factors influencing combustion, fire spread, and fire
504 consumption while previous wildfire models mainly focus on impacts of dead fuel moisture,
505 weather conditions on wildfire, fuel loads, and representation of live fuel moisture (Anderson &
506 Anderson 2010; Keeley et al. 2011; Jolly & Johnson 2018). The implications of this are that fire
507 potential will vary with plant water potential and uptake from soils, photosynthetic and
508 respiratory activity, carbon allocation and phenology with variability across species and over
509 time (Jolly & Johnson 2018). Therefore, future work to incorporate LFMC dynamics in wildfire
510 models could potentially play a vitally important role in the future studies of wildfire modeling
511 under climate change.

512 **5. Conclusions**

513 A hydrodynamic vegetation model, FATES-HYDRO, was used to estimate leaf water
514 status and thus LFMC dynamics of chaparral shrub species in southern California under
515 historical and future conditions. FATES-HYDRO model was validated using monthly mean
516 LFMC for three PFTs. The fire season length was projected to substantially increase under both
517 climate scenarios from 1960-1999 to 2080-2099. This could increase wildlife risk over time for
518 chaparral shrubs in southern California. Our results showed that temperature was the most

519 important driver of LFMC among all climatic variables. The LFMC estimated by the FATES-
520 HYDRO model offered a baseline of predicting plant hydraulic dynamics subjected to climate
521 change and provided a critical foundation that reductions in LFMC from climate warming may
522 exacerbate future wildfire risk. Longer fire season might have a significant impact on overall
523 public health and quality of life in the future.

524

525 *Data availability.* LFMC measurement data can be found in Pivovaroff et al. (2019). Species
526 abundance data can be found in Venturas et al. (2016). All other data are available within this
527 paper and in the Supplement.

528

529 *Supplement.* The supplement related to this article is available online at

530

531 *Author contributions.* WM, LZ, and CX were involved in designing the study. WM and CX
532 conducted the data analysis and ran model simulations. All authors contributed to writing,
533 reviewing, and improving the manuscript.

534

535 *Competing interests.* The authors declare that they have no conflict of interest.

536

537 *Acknowledgements.* We thank the editor Martin De Kauwe, the referee Douglas Kelley, and the
538 two anonymous referees for the improvement of this paper.

539

540 *Financial support.* This project is supported by the University of California Office of the
541 President Lab Fees Research Program and the Next Generation Ecosystem Experiment (NGEE)
542 Tropics, which is supported by the U.S. DOE Office of Science. CDK and JD are supported by
543 the DOE Office of Science, Regional and Global Model Analysis Program, Early Career
544 Research Program.

545

546 *Review statement.* This paper was edited by Martin De Kauwe, reviewed by the referee Douglas
547 Kelley, and the two anonymous referees.

548

549 **References**

550 Abatzoglou, J. T., and Brown, T. J.: A comparison of statistical downscaling methods suited for
551 wildfire applications, *Int. J. Climatol.*, 32, 772-780, <https://doi.org/10.1002/joc.2312>, 2012.

552 Abatzoglou, J. T.: Development of gridded surface meteorological data for ecological
553 applications and modelling, *Int. J. Climatol.*, 33, 121-131, <https://doi.org/10.1002/joc.3413>,
554 2013.

555 Agee, J. K., Wright, C. S., Williamson, N., and Huff, M. H.: Foliar moisture content of Pacific
556 Northwest vegetation and its relation to wildland fire behavior, *For. Ecol. Manag.*, 167, 57-66,
557 [https://doi.org/10.1016/S0378-1127\(01\)00690-9](https://doi.org/10.1016/S0378-1127(01)00690-9), 2002.

558 Anderson, S. A., and Anderson, W. R.: Ignition and fire spread thresholds in gorse (*Ulex*
559 *europaeus*), *Int. J. Wildland Fire.*, 19, 589-598, <https://doi.org/10.1071/WF09008>, 2010.

560 Aguado, I., Chuvieco, E., Boren, R., and Nieto, H.: Estimation of dead fuel moisture content
561 from meteorological data in Mediterranean areas. Applications in fire danger assessment, *Int. J.*
562 *Wildland Fire.*, 16, 390-397, <https://doi.org/10.1071/WF06136>, 2007.

563 Bistinas, I., Harrison, S. P., Prentice, I. C., and Pereira, J. M. C.: Causal relationships versus
564 emergent patterns in the global controls of fire frequency, *Biogeosciences*, 11, 5087-5101,
565 <https://doi.org/10.5194/bg-11-5087-2014>, 2014.

566 Burgan, R. E.: Estimating Live Fuel Moisture for the 1978 National Fire Danger Rating System,
567 Intermountain Forest and Range Experiment Station: Ogden, UT, USA, 1979.

568 Bilgili, E., and Saglam, B.: Fire behavior in maquis fuels in Turkey, *For. Ecol. Manag.*, 184,
569 201-207, [https://doi.org/10.1016/S0378-1127\(03\)00208-1](https://doi.org/10.1016/S0378-1127(03)00208-1), 2003.

570 Balch, J. K., Bradley, B. A., Abatzoglou, J. T., Nagy, R. C., Fusco, E. J., and Mahood, A. L.:
571 Human-started wildfires expand the fire niche across the United States, *Proc. Natl. Acad. Sci. U.*
572 *S. A.*, 114, 2946-2951, <https://doi.org/10.1073/pnas.1617394114>, 2017.

573 Bartlett, M. K., Scoffoni, C., and Sack, L.: The determinants of leaf turgor loss point and
574 prediction of drought tolerance of species and biomes: a global meta-analysis, *Ecol. Lett.*, 15,
575 393-405, <https://doi.org/10.1111/j.1461-0248.2012.01751.x>, 2012.

576 Bridges Jr, C. C.: Hierarchical cluster analysis, *Psychol. Rep.*, 18, 851-854,
577 <https://doi.org/10.2466/pr0.1966.18.3.851>, 1966.

578 Christoffersen, B. O., Gloor, M., Fauset, S., Fyllas, N. M., Galbraith, D. R., Baker, T. R., Kruijt,
579 B., Rowland, L., Fisher, R. A., Binks, O. J., and Sevanto, S.: Linking hydraulic traits to tropical

580 forest function in a size-structured and trait-driven model (TFS v. 1-Hydro), *Geosci. Model Dev.*,
581 9, 4227-4255, <https://doi.org/10.5194/gmd-9-4227-2016>, 2016.

582 Caccamo, G., Chisholm, L. A., Bradstock, R. A., and Puotinen, M. L.: Using remotely-sensed
583 fuel connectivity patterns as a tool for fire danger monitoring, *Geophys. Res. Lett.*, 39,
584 <https://doi.org/10.1029/2011GL050125>, 2012a.

585 Caccamo, G., Chisholm, L. A., Bradstock, R. A., Puotinen, M. L., and Phippen, B. G.: Monitoring
586 live fuel moisture content of heathland, shrubland and sclerophyll forest in south-eastern
587 Australia using MODIS data, *Int. J. Wildland Fire.*, 21, 257-269,
588 <http://dx.doi.org/10.1071/WF11024>, 2012b.

589 Clarke, H., Pitman, A. J., Kala, J., Carouge, C., Haverd, V., and Evans, J. P.: An investigation of
590 future fuel load and fire weather in Australia, *Clim. Change.*, 139, 591-605,
591 <http://dx.doi.org/10.1007/s10584-016-1808-9>, 2016.

592 Chuvieco, E., Cocero, D., Riano, D., Martin, P., Martinez-Vega, J., de la Riva, J., and Pérez, F.:
593 Combining NDVI and surface temperature for the estimation of live fuel moisture content in
594 forest fire danger rating, *Remote. Sens. Environ.*, 92, 322-331,
595 <https://doi.org/10.1016/j.rse.2004.01.019>, 2004.

596 Caldwell, P. M., Mametjanov, A., Tang, Q., Van Roekel, L. P., Golaz, J. C., Lin, W., Bader, D.
597 C., Keen, N. D., Feng, Y., Jacob, R., and Maltrud, M. E.: The DOE E3SM coupled model
598 version 1: Description and results at high resolution, *J. Adv. Model. Earth Syst.*, 11, 4095-4146,
599 <https://doi.org/10.1029/2019MS001870>, 2019.

600 Castro, F. X., Tudela, A., and Sebastià, M. T.: Modeling moisture content in shrubs to predict
601 fire risk in Catalonia (Spain), *Agric. For. Meteorol.*, 116, 49-59, [https://doi.org/10.1016/S0168-](https://doi.org/10.1016/S0168-1923(02)00248-4)
602 1923(02)00248-4, 2003.

603 Chuvieco, E., González, I., Verdú, F., Aguado, I., and Yebra, M.: Prediction of fire occurrence
604 from live fuel moisture content measurements in a Mediterranean ecosystem, *Int. J. Wildland*
605 *Fire.*, 18, 430-441, <https://doi.org/10.1071/WF08020>, 2009.

606 Collins, M., Knutti, R., Arblaster, J., Dufresne, J. L., Fichet, T., Friedlingstein, P., Gao, X.,
607 Gutowski, W. J., Johns, T., Krinner, G., and Shongwe, M.: Long-term climate change:
608 projections, commitments and irreversibility, In *Climate Change 2013-The Physical Science*
609 *Basis: Contribution of Working Group I to the Fifth Assessment Report of the Intergovernmental*
610 *Panel on Climate Change*. Cambridge University Press., 1029-1136, 2013.

611 Cook, B. I., Smerdon, J. E., Seager, R., and Coats, S.: Global warming and 21 st century drying,
612 *Clim. Dyn.*, 43, 2607-2627, <https://doi.org/10.1007/s00382-014-2075-y>, 2014.

613 Dennison, P. E., Moritz, M. A., and Taylor, R. S.: Evaluating predictive models of critical live
614 fuel moisture in the Santa Monica Mountains, California, *Int. J. Wildland. Fire.*, 17, 18-27,
615 <https://doi.org/10.1071/WF07017>, 2008.

616 Dennison, P. E., and Moritz, M. A.: Critical live fuel moisture in chaparral ecosystems: a
617 threshold for fire activity and its relationship to antecedent precipitation, *Int. J. Wildland. Fire.*,
618 18, 1021-1027, <https://doi.org/10.1071/WF08055>, 2009.

619 Dimitrakopoulos, A. P., and Papaioannou, K. K.: Flammability assessment of Mediterranean
620 forest fuels, *Fire. Technol.*, 37, 143-152, <https://doi.org/10.1023/A:1011641601076>, 2001.

621 Dai, A.: Increasing drought under global warming in observations and models, *Nat. Clim.*
622 *Change.*, 3, 52-58, <https://doi.org/10.1038/nclimate1633>, 2013.

623 Duursma, R. A., and Medlyn, B. E.: MAESPA: a model to study interactions between water
624 limitation, environmental drivers and vegetation function at tree and stand levels, with an
625 example application to [CO₂]×drought interactions, *Geosci. Model. Dev.*, 5, 919-940,
626 <https://doi.org/10.5194/gmd-5-919-2012>, 2012.

627 Flannigan, M. D., Krawchuk, M. A., de Groot, W. J., Wotton, B. M., and Gowman, L. M.:
628 Implications of changing climate for global wildland fire, *Int. J. Wildland. Fire.*, 18, 483-507,
629 <https://doi.org/10.1071/WF08187>, 2009.

630 Fisher, R. A., Williams, M., Da Costa, A. L., Malhi, Y., Da Costa, R. F., Almeida, S., and Meir,
631 P.: The response of an Eastern Amazonian rain forest to drought stress: results and modelling
632 analyses from a throughfall exclusion experiment, *Glob. Change. Biol.*, 13, 2361-2378,
633 <https://doi.org/10.1111/j.1365-2486.2007.01417.x>, 2007.

634 Fisher, R. A., Muszala, S., Versteinstein, M., Lawrence, P., Xu, C., McDowell, N. G., Knox, R.
635 G., Koven, C., Holm, J., Rogers, B. M., and Spessa, A.: Taking off the training wheels: the
636 properties of a dynamic vegetation model without climate envelopes, *CLM4. 5 (ED)*, *Geosci.*
637 *Model Dev.*, 8, 3593-3619, <https://doi.org/10.5194/gmd-8-3593-2015>, 2015.

638 Fisher, R. A., Koven, C. D., Anderegg, W. R., Christoffersen, B. O., Dietze, M. C., Farnior, C.
639 E., Holm, J. A., Hurtt, G. C., Knox, R. G., Lawrence, P. J., and Lichstein, J. W.: Vegetation
640 demographics in Earth System Models: A review of progress and priorities, *Glob. Change. Biol.*,
641 24, 35-54, <https://doi.org/10.1111/gcb.13910>, 2018.

642 Gillett, N. P., Weaver, A. J., Zwiers, F. W., and Flannigan, M. D.: Detecting the effect of climate
643 change on Canadian forest fires, *Geophys. Res. Lett.*, 31,
644 <https://doi.org/10.1029/2004GL020876>, 2004.

645 Goss, M., Swain, D. L., Abatzoglou, J. T., Sarhadi, A., Kolden, C. A., Williams, A. P., and
646 Diffenbaugh, N. S.: Climate change is increasing the likelihood of extreme autumn wildfire
647 conditions across California, *Environ. Res. Lett.*, 15, 094016, [https://doi.org/10.1088/1748-](https://doi.org/10.1088/1748-9326/ab83a7)
648 [9326/ab83a7](https://doi.org/10.1088/1748-9326/ab83a7), 2020.

649 Hantson, S., Arneeth, A., Harrison, S. P., Kelley, D. I., Prentice, I. C., Rabin, S. S., Archibald, S.,
650 Mouillot, F., Arnold, S. R., Artaxo, P., and Bachelet, D.: The status and challenge of global fire
651 modelling, *Biogeosciences*, 13, 3359-3375, <https://doi.org/10.5194/bg-13-3359-2016>, 2016.

652 Holm, J. A., Shugart, H. H., Van Bloem, S. J., and Larocque, G. R.: Gap model development,
653 validation, and application to succession of secondary subtropical dry forests of Puerto Rico,
654 *Ecol. Modell.*, 233, 70-82, <https://doi.org/10.1016/j.ecolmodel.2012.03.014>, 2012.

655 Jacobsen, A. L., Pratt, R. B., Davis, S. D., and Ewers, F. W.: Comparative community
656 physiology: nonconvergence in water relations among three semi-arid shrub communities, *New.*
657 *Phytol.*, 180, 100-113, <https://doi.org/10.1111/j.1469-8137.2008.02554.x>, 2008.

658 Jolly, W. M., and Johnson, D. M.: Pyro-ecophysiology: shifting the paradigm of live wildland
659 fuel research, *Fire*, 1, 8, <https://doi.org/10.3390/fire1010008>, 2018.

660 Jackson, D. A.: Stopping rules in principal components analysis: a comparison of heuristical and
661 statistical approaches, *Ecology*, 74, 2204-2214, <https://doi.org/10.2307/1939574>, 1993.

662 Kelley, D. I., Bistinas, I., Whitley, R., Burton, C., Marthews, T. R., and Dong, N.: How
663 contemporary bioclimatic and human controls change global fire regimes, *Nat. Clim. Change.*, 9,
664 690-696, <https://doi.org/10.1038/s41558-019-0540-7>, 2019.

665 Konings, A. G., Rao, K., and Steele-Dunne, S. C.: Macro to micro: microwave remote sensing of
666 plant water content for physiology and ecology, *New. Phytol.*, 223, 1166-1172,
667 <https://doi.org/10.1111/nph.15808>, 2019.

668 Keeley, J. E.: Future of California floristics and systematics: wildfire threats to the California
669 flora, *Madrono*, 175-179, 1995.

670 Keeley, J. E., and Zedler, P. H.: Large, high-intensity fire events in southern California
671 shrublands: debunking the fine-grain age patch model, *Ecol. Appl.*, 19, 69-94,
672 <https://doi.org/10.1890/1073-0107-0281.1>, 2009.

673 Keeley, J. E., Bond, W. J., Bradstock, R. A., Pausas, J. G., and Rundel, P. W.: Fire in
674 Mediterranean ecosystems: ecology, evolution and management, Cambridge University Press,
675 <https://doi.org/10.1017/9781107301633>, 2011.

676 Kennedy, D., Swenson, S., Oleson, K. W., Lawrence, D. M., Fisher, R., Lola da Costa, A. C.,
677 and Gentine, P.: Implementing plant hydraulics in the community land model, version 5, *J. Adv.
678 Model. Earth Syst.*, 11, 485-513, <https://doi.org/10.1029/2018MS001500>, 2019.

679 Koven, C. D., Knox, R. G., Fisher, R. A., Chambers, J. Q., Christoffersen, B. O., Davies, S. J.,
680 Detto, M., Dietze, M. C., Faybishenko, B., Holm, J., and Huang, M.: Benchmarking and
681 parameter sensitivity of physiological and vegetation dynamics using the Functionally
682 Assembled Terrestrial Ecosystem Simulator (FATES) at Barro Colorado Island, Panama,
683 *Biogeosciences*, 17, 3017-3044, <https://doi.org/10.5194/bg-17-3017-2020>, 2020.

684 Krawchuk, M. A., Moritz, M. A., Parisien, M. A., Van Dorn, J., and Hayhoe, K.: Global
685 pyrogeography: the current and future distribution of wildfire, *Plos One*, 4, e5102,
686 <https://doi.org/10.1371/journal.pone.0005102>, 2009.

687 Linn, R., Reisner, J., Colman, J. J., and Winterkamp, J.: Studying wildfire behavior using
688 FIRETEC, *Int. J. Wildland. Fire.*, 11, 233-246, <https://doi.org/10.1071/WF02007>, 2002.

689 Liu, Y., Stanturf, J., and Goodrick, S.: Trends in global wildfire potential in a changing climate,
690 *For. Ecol. Manag.*, 259, 685-697, <https://doi.org/10.1016/j.foreco.2009.09.002>, 2010.

691 Massoud, E. C., Xu, C., Fisher, R. A., Knox, R. G., Walker, A. P., Serbin, S. P., Christoffersen,
692 B. O., Holm, J. A., Kueppers, L. M., Ricciuto, D. M., and Wei, L.: Identification of key
693 parameters controlling demographically structured vegetation dynamics in a land surface model:
694 CLM4. 5 (FATES), *Geosci. Model Dev.*, 12, 4133-4164, [https://doi.org/10.5194/gmd-12-4133-](https://doi.org/10.5194/gmd-12-4133-2019)
695 2019, 2019.

696 Moorcroft, P. R., Hurtt, G. C., and Pacala, S. W.: A method for scaling vegetation dynamics: the
697 ecosystem demography model (ED), *Ecol. Monogr.*, 71, 557-586, [https://doi.org/10.1890/0012-](https://doi.org/10.1890/0012-9615(2001)071[0557:AMFSVD]2.0.CO;2)
698 9615(2001)071[0557:AMFSVD]2.0.CO;2, 2001.

699 Mikkelsen, T. N., Beier, C., Jonasson, S., Holmstrup, M., Schmidt, I. K., Ambus, P., Pilegaard,
700 K., Michelsen, A., Albert, K., Andresen, L. C., and Arndal, M. F.: Experimental design of
701 multifactor climate change experiments with elevated CO₂, warming and drought: the
702 CLIMAITE project, *Funct. Ecol.*, 22, 185-195, [https://doi.org/10.1111/j.1365-](https://doi.org/10.1111/j.1365-2435.2007.01362.x)
703 2435.2007.01362.x, 2008.

704 Moritz, M. A., Parisien, M. A., Batllori, E., Krawchuk, M. A., Van Dorn, J., Ganz, D. J., and
705 Hayhoe, K.: Climate change and disruptions to global fire activity, *Ecosphere*, 3, 1-22,
706 <https://doi.org/10.1890/ES11-00345.1>, 2012.

707 McDowell, N. G., Fisher, R. A., Xu, C., Domec, J. C., Hölttä, T., Mackay, D. S., Sperry, J. S.,
708 Boutz, A., Dickman, L., Gehres, N., and Limousin, J. M.: Evaluating theories of drought-induced
709 vegetation mortality using a multimodel–experiment framework, *New. Phytol.*, 200, 304-321,
710 <https://doi.org/10.1111/nph.12465>, 2013.

711 Mencuccini, M., Manzoni, S., and Christoffersen, B.: Modelling water fluxes in plants: from
712 tissues to biosphere, *New. Phytol.*, 222, 1207-1222, <https://doi.org/10.1111/nph.15681>, 2019.

713 Matthews, S., Sullivan, A. L., Watson, P., and Williams, R. J.: Climate change, fuel and fire
714 behaviour in a eucalypt forest, *Glob. Change Biol.*, 18, 3212-3223,
715 <https://doi.org/10.1111/j.1365-2486.2012.02768.x>, 2012.

716 Manabe, S., and Wetherald, R. T.: The effects of doubling the CO₂ concentration on the climate
717 of a general circulation model, *Int. J. Atmos. Sci.*, 32, 3-15, [https://doi.org/10.1175/1520-0469\(1975\)032<0003:TEODTC>2.0.CO;2](https://doi.org/10.1175/1520-0469(1975)032<0003:TEODTC>2.0.CO;2), 1975.

719 Meinzer, F. C., James, S. A., Goldstein, G., and Woodruff, D.: Whole-tree water transport scales
720 with sapwood capacitance in tropical forest canopy trees, *Plant. Cell. Environ.*, 26, 1147-1155,
721 <https://doi.org/10.1046/j.1365-3040.2003.01039.x>, 2003.

722 Meinzer, F. C., Johnson, D. M., Lachenbruch, B., McCulloh, K. A., and Woodruff, D. R.: Xylem
723 hydraulic safety margins in woody plants: coordination of stomatal control of xylem tension with
724 hydraulic capacitance, *Funct. Ecol.*, 23, 922-930, <https://doi.org/10.1111/j.1365-2435.2009.01577.x>, 2009.

726 Meinshausen, M., Smith, S. J., Calvin, K., Daniel, J. S., Kainuma, M. L., Lamarque, J. F.,
727 Matsumoto, K., Montzka, S. A., Raper, S. C., Riahi, K., and Thomson, A. G.: The RCP
728 greenhouse gas concentrations and their extensions from 1765 to 2300, *Clim. Change.*, 109, 213-
729 241, <http://dx.doi.org/10.1007/s10584-011-0156-z>, 2011.

730 Nolan, R. H., Boer, M. M., Resco de Dios, V., Caccamo, G., and Bradstock, R. A.: Large-scale,
731 dynamic transformations in fuel moisture drive wildfire activity across southeastern Australia,
732 *Geophys. Res. Lett.*, 43, 4229-4238, <https://doi.org/10.1002/2016GL068614>, 2016.

733 Nolan, R. H., Blackman, C. J., de Dios, V. R., Choat, B., Medlyn, B. E., Li, X., Bradstock, R. A.,
734 and Boer, M. M.: Linking forest flammability and plant vulnerability to drought, *Forests*, 11,
735 779, <https://doi.org/10.3390/f11070779>, 2020.

736 National Fuel Moisture Database.
737 [https://www.wfas.net/nfmd/public/site.php?site_fuel=Stunt%20Road%2C%20Calabasas&gacc=](https://www.wfas.net/nfmd/public/site.php?site_fuel=Stunt%20Road%2C%20Calabasas&gacc=SOCC&state=CA&grup=LA%20County&sitefuel=site&display_type=Table%20Only%20Actual%20Data&fuel_selected=Chamise)
738 [SOCC&state=CA&grup=LA%20County&sitefuel=site&display_type=Table%20Only%20Actual%20Data&fuel_selected=Chamise](https://www.wfas.net/nfmd/public/site.php?site_fuel=Stunt%20Road%2C%20Calabasas&gacc=SOCC&state=CA&grup=LA%20County&sitefuel=site&display_type=Table%20Only%20Actual%20Data&fuel_selected=Chamise), 2021.

740 Pivovarov, A. L., Emery, N., Sharifi, M. R., Witter, M., Keeley, J. E., and Rundel, P. W.: The
741 effect of ecophysiological traits on live fuel moisture content, *Fire*, 2, 28,
742 <https://doi.org/10.3390/fire2020028>, 2019.

743 Powell, T. L., Koven, C. D., Johnson, D. J., Faybishenko, B., Fisher, R. A., Knox, R. G.,
744 McDowell, N. G., Condit, R., Hubbell, S. P., Wright, S. J., and Chambers, J. Q.: Variation in
745 hydroclimate sustains tropical forest biomass and promotes functional diversity, *New Phytol.*,
746 219, 932-946, <https://doi.org/10.1111/nph.15271>, 2018.

747 Pellizzaro, G., Cesaraccio, C., Duce, P., Ventura, A., and Zara, P.: Relationships between
748 seasonal patterns of live fuel moisture and meteorological drought indices for Mediterranean
749 shrubland species, *Int. J. Wildland. Fire.*, 16, 232-241, <https://doi.org/10.1071/WF06081>, 2007.

750 Plucinski, M. P.: The investigation of factors governing ignition and development of fires in
751 heathland vegetation, PhD thesis. University of New South Wales, Sydney. 2003.

752 Pimont, F., Ruffault, J., Martin-StPaul, N. K., and Dupuy, J. L.: Why is the effect of live fuel
753 moisture content on fire rate of spread underestimated in field experiments in shrublands?, *Int. J.*
754 *Wildland. Fire.*, 28, 127-137, <https://doi.org/10.1071/WF18056>, 2019.

755 Pataki, D. E., Huxman, T. E., Jordan, D. N., Zitzer, S. F., Coleman, J. S., Smith, S. D., Nowak,
756 R. S., and Seemann, J. R.: Water use of two Mojave Desert shrubs under elevated CO₂, *Glob.*
757 *Change Biol.*, 6, 889-897, <https://doi.org/10.1046/j.1365-2486.2000.00360.x>, 2000.

758 Pineda-Garcia, F., Paz, H., and Meinzer, F. C.: Drought resistance in early and late secondary
759 successional species from a tropical dry forest: the interplay between xylem resistance to
760 embolism, sapwood water storage and leaf shedding, *Plant. Cell. Environ.*, 36, 405-418,
761 <https://doi.org/10.1111/j.1365-3040.2012.02582.x>, 2013.

762 Rabin, S. S., Melton, J. R., Lasslop, G., Bachelet, D., Forrest, M., Hantson, S., Kaplan, J. O., Li,
763 F., Mangeon, S., Ward, D. S., and Yue, C.: The Fire Modeling Intercomparison Project
764 (FireMIP), phase 1: experimental and analytical protocols with detailed model descriptions,
765 *Geosci. Model Dev.*, 10, 1175-1197, <https://doi.org/10.5194/gmd-10-1175-2017>, 2017.

766 Rossa, C. G., and Fernandes, P. M.: Live fuel moisture content: The ‘pea under the mattress’ of
767 fire spread rate modeling?, *Fire*, 1, 43, <https://doi.org/10.3390/fire1030043>, 2018.

768 Rind, D., Goldberg, R., Hansen, J., Rosenzweig, C., and Ruedy, R.: Potential evapotranspiration
769 and the likelihood of future drought, *J. Geophys. Res. Atmos.*, 95, 9983-10004,
770 <https://doi.org/10.1029/JD095iD07p09983>, 1990.

771 Rothermel, R. C.: A mathematical model for predicting fire spread in wildland fuels (Vol. 115),
772 Intermountain Forest & Range Experiment Station, Forest Service, US Department of
773 Agriculture, 1972.

774 Ruthrof, K. X., Fontaine, J. B., Matusick, G., Breshears, D. D., Law, D. J., Powell, S., and
775 Hardy, G.: How drought-induced forest die-off alters microclimate and increases fuel loadings
776 and fire potentials, *Int. J. Wildland Fire.*, 25, 819-830, <https://doi.org/10.1071/WF15028>, 2016.

777 Sturtevant, B. R., Scheller, R. M., Miranda, B. R., Shinneman, D., and Syphard, A.: Simulating
778 dynamic and mixed-severity fire regimes: a process-based fire extension for LANDIS-II, *Ecol.*
779 *Modell.*, 220, 3380-3393, <https://doi.org/10.1016/j.ecolmodel.2009.07.030>, 2009.

780 Stocks, B. J., Fosberg, M. A., Lynham, T. J., Mearns, L., Wotton, B. M., Yang, Q., Jin, J. Z.,
781 Lawrence, K., Hartley, G. R., Mason, J. A., and McKenney, D. W.: Climate change and forest
782 fire potential in Russian and Canadian boreal forests, *Clim. Change.*, 38, 1-13,
783 <https://doi.org/10.1023/A:1005306001055>, 1998.

784 Schroeder, M. J., Glovinsky, M., Henricks, V. F., Hood, F. C., and Hull, M. K.: Synoptic
785 weather types associated with critical fire weather, USDA Forest Service, Pacific Southwest
786 Range and Experiment Station. Berkeley, CA. 1964.

787 Seiler, C., Hutjes, R. W. A., Kruijt, B., Quispe, J., Añez, S., Arora, V. K., Melton, J. R., Hickler,
788 T., and Kabat, P.: Modeling forest dynamics along climate gradients in Bolivia, *J. Geophys. Res.*
789 *Biogeosci.*, 119, 758-775, <https://doi.org/10.1002/2013JG002509>, 2014.

790 Sheffield, J., and Wood, E. F.: Projected changes in drought occurrence under future global
791 warming from multi-model, multi-scenario, IPCC AR4 simulations, *Clim. Dyn.*, 31, 79-105,
792 <https://doi.org/10.1007/s00382-007-0340-z>, 2008.

793 Saura-Mas, S., and Lloret, F.: Leaf and shoot water content and leaf dry matter content of
794 Mediterranean woody species with different post-fire regenerative strategies, *Ann. Bot.*, 99, 545-
795 554, <https://doi.org/10.1093/aob/mcl284>, 2007.

796 Sun, W., Maseyk, K., Lett, C., and Seibt, U.: Litter dominates surface fluxes of carbonyl sulfide
797 in a Californian oak woodland, *J. Geophys. Res. Biogeosci.*, 121, 438-450,
798 <https://doi.org/10.1002/2015JG003149>, 2016.

799 Thonicke, K., Spessa, A., Prentice, I. C., Harrison, S. P., Dong, L., and Carmona-Moreno, C.:
800 The influence of vegetation, fire spread and fire behaviour on biomass burning and trace gas
801 emissions: results from a process-based model, *Biogeosciences*, 7, 1991-2011,
802 <https://doi.org/10.5194/bg-7-1991-2010>, 2010.

803 Tyree, M. T., and Hammel, H. T.: The measurement of the turgor pressure and the water
804 relations of plants by the pressure-bomb technique, *J. Exp. Bot.*, 23, 267-282,
805 <https://doi.org/10.1093/jxb/23.1.267>, 1972.

806 Tyree, M. T., and Yang, S.: Water-storage capacity of Thuja, Tsuga and Acer stems measured by
807 dehydration isotherms, *Planta*, 182, 420-426, <https://doi.org/10.1007/BF02411394>, 1990.

808 Tognetti, R., Minnocci, A., Peñuelas, J., Raschi, A., and Jones, M. B.: Comparative field water
809 relations of three Mediterranean shrub species co-occurring at a natural CO₂ vent, *J. Exp. Bot.*,
810 51, 1135-1146, <https://doi.org/10.1093/jexbot/51.347.1135>, 2000.

811 Tjiputra, J. F., Roelandt, C., Bentsen, M., Lawrence, D. M., Lorentzen, T., Schwinger, J., Seland,
812 Ø., and Heinze, C.: Evaluation of the carbon cycle components in the Norwegian Earth System
813 Model (NorESM), *Geosci. Model Dev.*, 6, 301-325, <https://doi.org/10.5194/gmd-6-301-2013>,
814 2013.

815 Venturas, M. D., MacKinnon, E. D., Dario, H. L., Jacobsen, A. L., Pratt, R. B., and Davis, S. D.:
816 Chaparral shrub hydraulic traits, size, and life history types relate to species mortality during
817 California's historic drought of 2014, *Plos One*, 11,
818 <https://doi.org/10.1371/journal.pone.0159145>, 2016.

819 Veblen, T. T., Kitzberger, T., and Donnegan, J.: Climatic and human influences on fire regimes
820 in ponderosa pine forests in the Colorado Front Range, *Ecol. Appl.*, 10, 1178-1195,
821 [https://doi.org/10.1890/1051-0761\(2000\)010\[1178:CAHIOF\]2.0.CO;2](https://doi.org/10.1890/1051-0761(2000)010[1178:CAHIOF]2.0.CO;2), 2000.

822 Westerling, A. L., Gershunov, A., Brown, T. J., Cayan, D. R., and Dettinger, M. D.: Climate and
823 wildfire in the western United States, *Bull. Am. Meteorol. Soc.*, 84, 595-604,
824 <https://doi.org/10.1175/BAMS-84-5-595>, 2003.

825 Westerling, A. L., Hidalgo, H. G., Cayan, D. R., and Swetnam, T. W.: Warming and earlier
826 spring increase western US forest wildfire activity, *Science*, 313, 940-943,
827 <https://doi.org/10.1098/rstb.2015.0178>, 2006.

828 Williams, A. P., Abatzoglou, J. T., Gershunov, A., Guzman-Morales, J., Bishop, D. A., Balch, J.
829 K., and Lettenmaier, D. P.: Observed impacts of anthropogenic climate change on wildfire in
830 California, *Earths. Future.*, 7, 892-910, <https://doi.org/10.1029/2019EF001210>, 2019.

831 Wullschleger, S. D., Gunderson, C. A., Hanson, P. J., Wilson, K. B., and Norby, R. J.:
832 Sensitivity of stomatal and canopy conductance to elevated CO₂ concentration—interacting

833 variables and perspectives of scale, *New Phytol.*, 153, 485-496, <https://doi.org/10.1046/j.0028->
834 646X.2001.00333.x, 2002.

835 Wu, J., Serbin, S. P., Ely, K. S., Wolfe, B. T., Dickman, L. T., Grossiord, C., Michaletz, S. T.,
836 Collins, A. D., Detto, M., McDowell, N. G., and Wright, S. J.: The response of stomatal
837 conductance to seasonal drought in tropical forests, *Glob. Change Biol.*, 26, 823-839,
838 <https://doi.org/10.1111/gcb.14820>, 2020.

839 Wei, L., Xu, C., Jansen, S., Zhou, H., Christoffersen, B. O., Pockman, W. T., Middleton, R. S.,
840 Marshall, J. D., and McDowell, N. G.: A heuristic classification of woody plants based on
841 contrasting shade and drought strategies, *Tree. Physiol.*, 39, 767-781,
842 <https://doi.org/10.1093/treephys/tpy146>, 2019.

843 Xu, C., McDowell, N. G., Sevanto, S., and Fisher, R. A.: Our limited ability to predict vegetation
844 dynamics under water stress, *New. Phytol.*, 200, 298-300, <https://doi.org/10.1111/nph.12450>,
845 2013.

846 Xu, X., Medvigy, D., Powers, J. S., Becknell, J. M., and Guan, K.: Diversity in plant hydraulic
847 traits explains seasonal and inter-annual variations of vegetation dynamics in seasonally dry
848 tropical forests, *New. Phytol.*, 212, 80-95, <https://doi.org/10.1111/nph.14009>, 2016.

849 Xu, C., McDowell, N. G., Fisher, R. A., Wei, L., Sevanto, S., Christoffersen, B. O., Weng, E.,
850 and Middleton, R. S.: Increasing impacts of extreme droughts on vegetation productivity under
851 climate change, *Nat. Clim. Change.*, 9, 948-953, <https://doi.org/10.1038/s41558-019-0630-6>,
852 2019.

853 Yebra, M., Chuvieco, E., and Riaño, D.: Estimation of live fuel moisture content from MODIS
854 images for fire risk assessment, *Agric. For. Meteorol.*, 148, 523-536,
855 <https://doi.org/10.1016/j.agrformet.2007.12.005>, 2008.

856 Yebra, M., Dennison, P. E., Chuvieco, E., Riano, D., Zylstra, P., Hunt Jr, E. R., Danson, F. M.,
857 Qi, Y., and Jurdao, S.: A global review of remote sensing of live fuel moisture content for fire
858 danger assessment: Moving towards operational products, *Remote. Sens. Environ.*, 136, 455-
859 468, <https://doi.org/10.1016/j.rse.2013.05.029>, 2013.

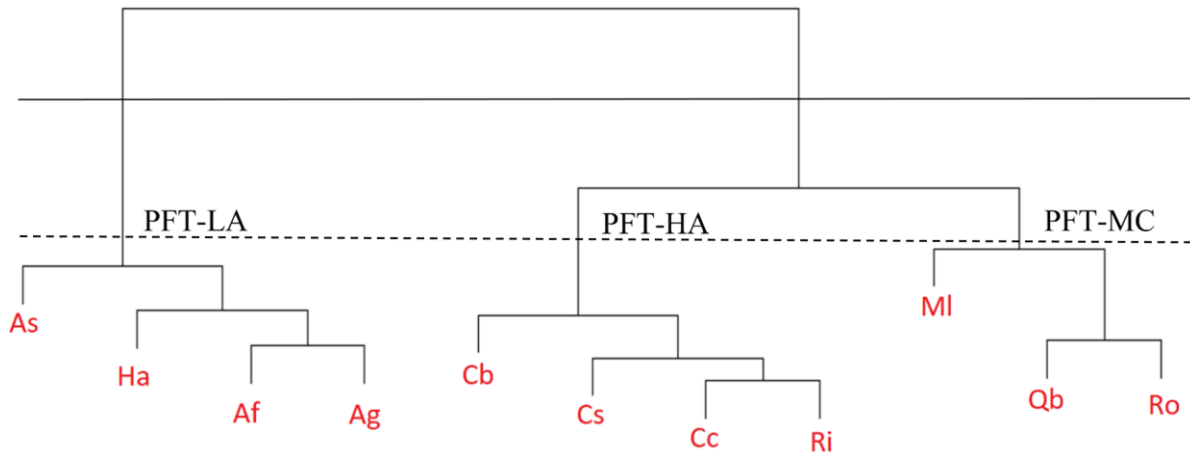
860 Yebra, M., Quan, X., Riaño, D., Larraondo, P. R., van Dijk, A. I., and Cary, G. J.: A fuel
861 moisture content and flammability monitoring methodology for continental Australia based on
862 optical remote sensing, *Remote. Sens. Environ.*, 212, 260-272, [https://](https://doi.org/10.4225/41/5837cd92ada9f)
863 doi.org/10.4225/41/5837cd92ada9f, 2018.

864 Zarco-Tejada, P. J., Rueda, C. A., and Ustin, S. L.: Water content estimation in vegetation with
865 MODIS reflectance data and model inversion methods, *Remote. Sens. Environ.*, 85, 109-124,
866 [https://doi.org/10.1016/S0034-4257\(02\)00197-9](https://doi.org/10.1016/S0034-4257(02)00197-9), 2003.

867 Zhao, T., and Dai, A.: The magnitude and causes of global drought changes in the twenty-first
868 century under a low–moderate emissions scenario, *J. Clim.*, 28, 4490-4512,
869 <https://doi.org/10.1175/JCLI-D-14-00363.1>, 2015.

870

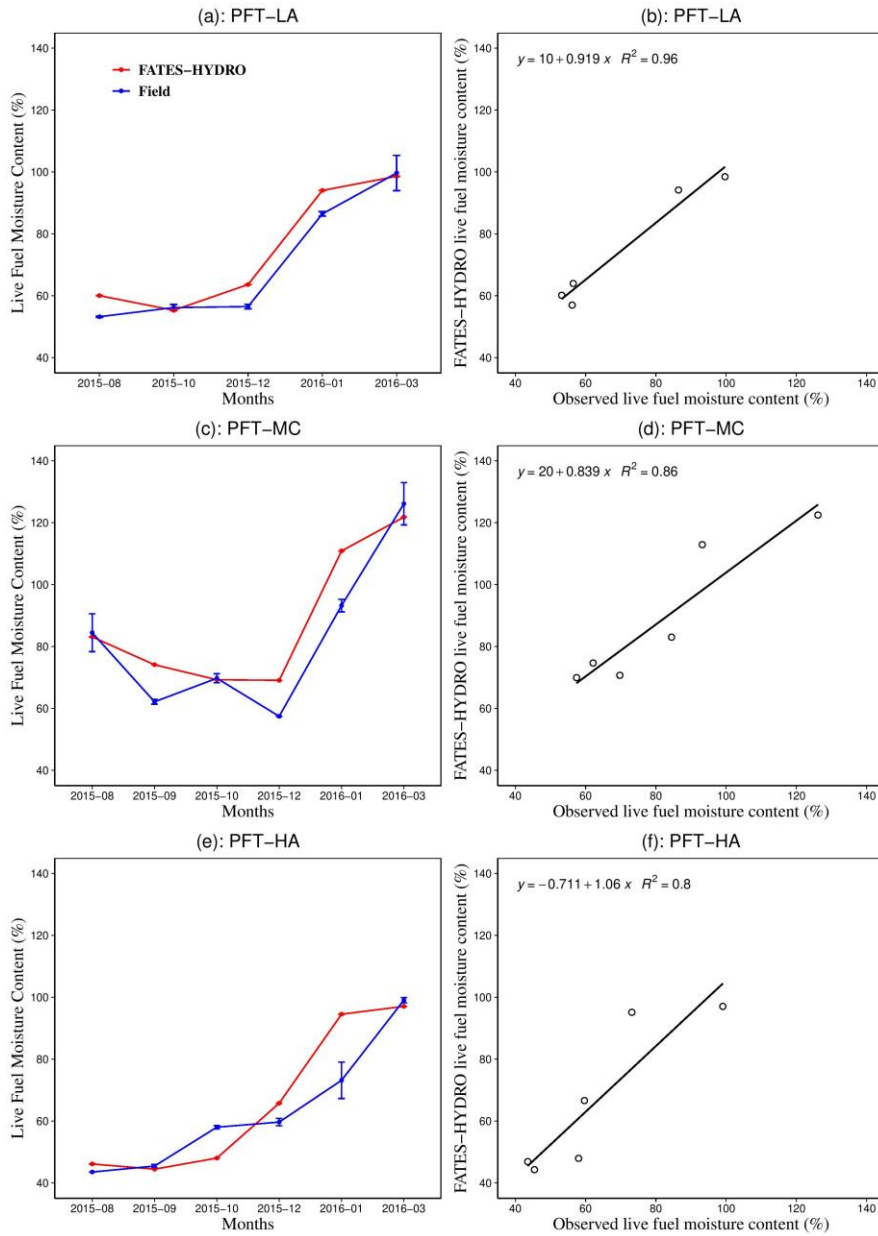
871



872

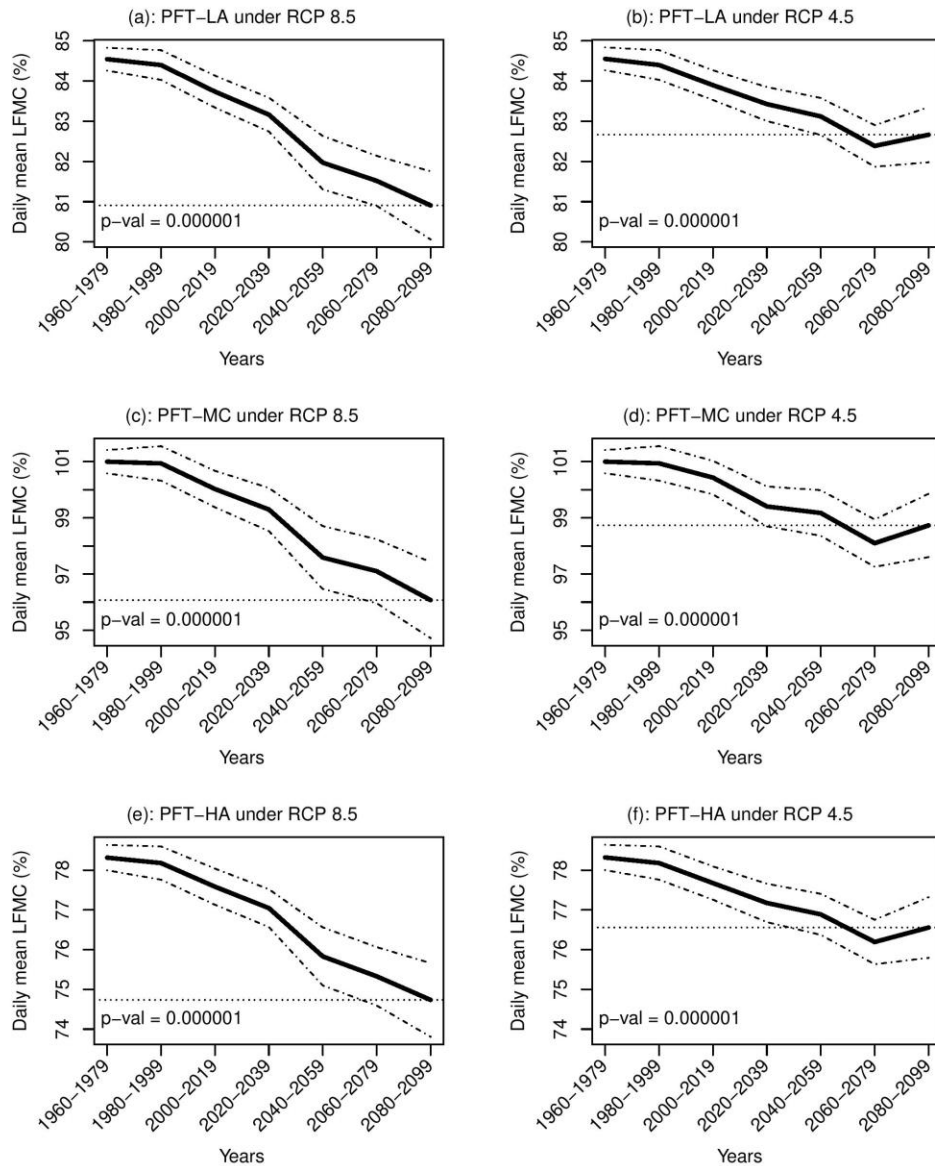
873 **Fig 1.** Hierarchical cluster analysis of allometry and hydraulic traits for eleven chaparral shrub
 874 species used to define three plant functional types at Stunt Ranch. The plant functional types
 875 with a low productivity and an aggressive drought tolerance hydraulic strategy (PFT-LA) was
 876 defined based on traits of red shank (*Adenostoma sparsifolium* - As), toyon (*Heteromeles*
 877 *arbutifolia* - Ha), chamise (*Adenostoma fasciculatum* - Af), big berry manzanita (*Arctostaphylos*
 878 *glauca* - Ag); the plant functional types with a high productivity and an aggressive drought
 879 tolerance hydraulic strategy (PFT-HA) was defined based on traits of mountain mahogany
 880 (*Cercocarpus betuloides* - Cb), greenbark ceanothus (*Ceanothus spinosus* - Cs), buck brush
 881 (*Ceanothus cuneatus* - Cc), hollyleaf redberry (*Rhamnus ilicifolia* - Ri); the plant functional
 882 types with a medium productivity and an conservative drought tolerance hydraulic strategy
 883 (PFT-MC) was defined based on traits of laurel sumac (*Malosma laurina* - MI), scrub oak
 884 (*Quercus berberidifolia* - Qb), sugar bush (*Rhus ovata* - Ro).

885



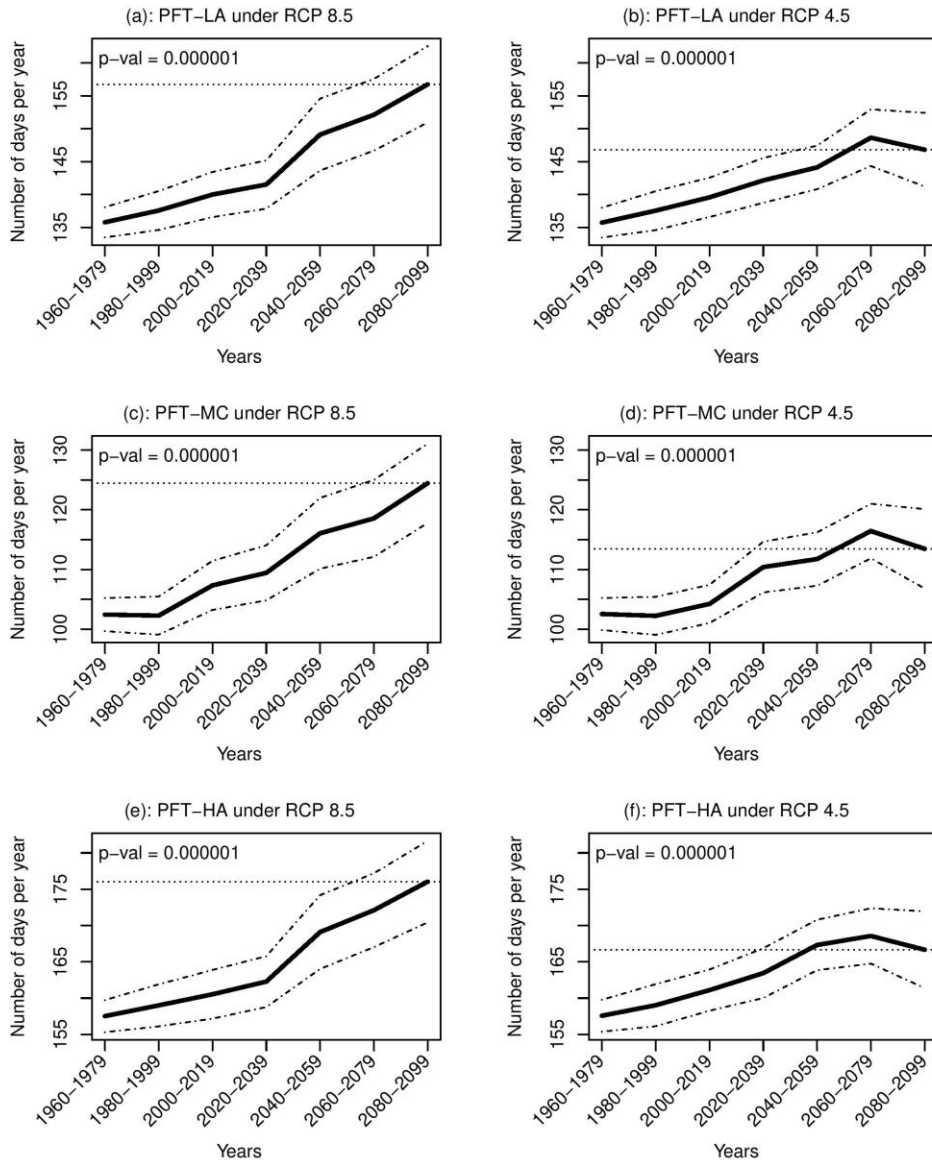
886

887 **Fig.2** Simulated and observed monthly live fuel moisture content and related R^2 values for three
 888 PFTs (refer to Figure 1 for explanation of the PFTs).



889

890 **Fig.3** Temporal changes in daily mean live fuel moisture content (black solid line) and 95%
 891 confidence interval (black dash-dot line) from 1960 to 2099 for three PFTs (refer to Figure 1 for
 892 explanation of the PFTs) under climate scenario RCP 4.5 and 8.5 with 20 Earth System Models
 893 considering all climatic variables changes. The P values were calculated using bootstrap
 894 sampling to test whether the daily mean live fuel moisture content across different models during
 895 the future period (2080–2099) was significantly lower than that during the historical period
 896 (1960-1999). The grey horizontal dotted line represents the ensemble mean for 2080–2099.

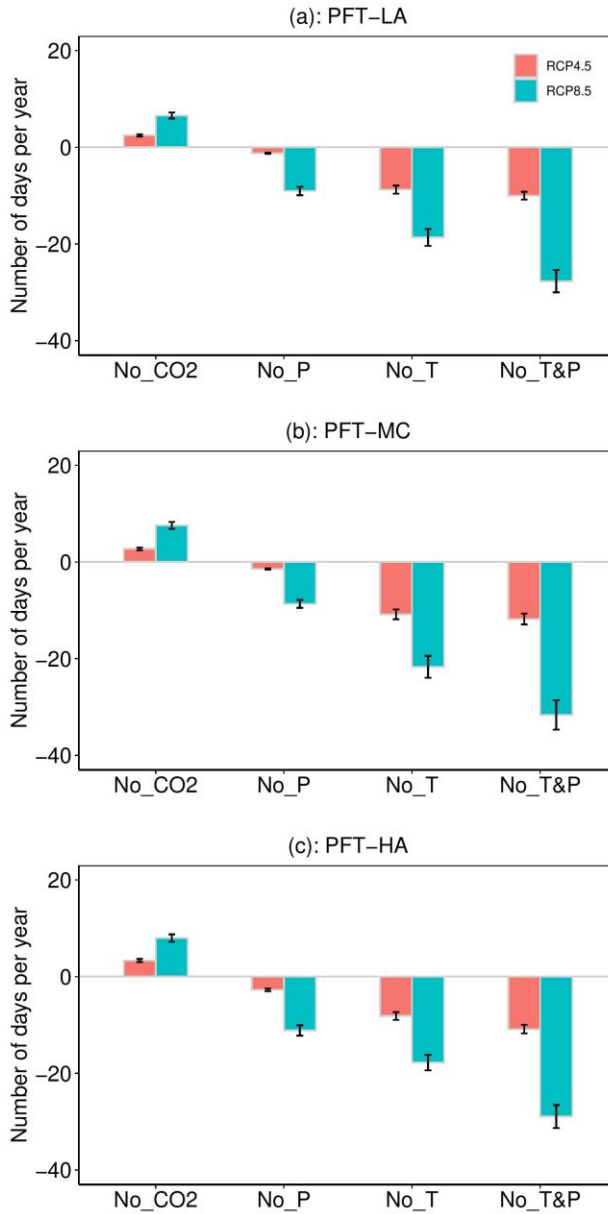


897

898 **Fig.4** Temporal changes in average number of days per year of live fuel moisture content below
 899 79% (black solid line) and 95% confidence interval (black dash-dot line) from 1960 to 2099 for
 900 three PFTs (refer to Figure 1 for explanation of the PFTs) under climate scenario RCP 4.5 and
 901 8.5 with 20 Earth System Models considering all climatic variables changes. The P values were
 902 calculated using bootstrap sampling to test whether the number of days across different models
 903 during the future period (2080–2099) was significantly higher than that during the historical
 904 period (1960-1999). The grey horizontal dotted line represents the ensemble mean for 2080–
 905 2099.

906

907



908

909 **Fig.5** Differences on number of days per year of live fuel moisture content below 79% from
 910 2080 to 2099 for three PFTs (refer to Figure 1 for explanation of the PFTs) under climate
 911 scenario RCP 4.5 and 8.5 between considering all climatic variables changes and without
 912 considering CO₂, precipitation, temperature, and precipitation & temperature changes.